Irregular bodies of non-welded Amalia Tuff within the Pena Tank Rhyolite, western San Luis Basin, north-central NM

William C. McIntosh, Daniel J. Koning, and Matt Zimmerer, 2011, pp. 223-234
Supplemental data available: http://nmgs.nmt.edu/repository/index.cfm?rid=2011002
in:
Geology of the Tusas Mountains and Ojo Caliente, Author Koning, Daniel J.; Karlstrom, Karl E.; Kelley, Shari A.; Lueth, Virgil W.; Aby, Scott B., New Mexico Geological Society 62nd Annual Fall Field Conference Guidebook, 418 p.

This page is intentionally left blank to maintain order of facing pages.

IRREGULAR BODIES OF NON-WELDED AMALIA TUFF WITHIN THE PEÑA TANK RHYOLITE, WESTERN SAN LUIS BASIN, NORTH-CENTRAL NEW MEXICO

WILLIAM C. MCINTOSH[1], DANIEL J. KONING[1], AND MATT ZIMMERER[2]
[1]New Mexico Bureau of Geology and Mineral Resources, New Mexico Institute of Mining and Technology, Socorro, NM 87801; mcintosh@nmt.edu,
[2]Department of Earth and Environmental Sciences, New Mexico Institute of Mining and Technology, Socorro, NM 87801

Abstract—The Peña Tank Rhyolite flow complex (new name) in north-central New Mexico consists of red-gray rhyolite lava that contains numerous, irregular bodies of white rhyolite, ranging from 3 m to 400 m in diameter. The two lithologies show outcrop-scale textures similar to those seen in co-mingled magmas, with fragments of red-gray lava included in the white rhyolite and veins of white rhyolite penetrating the red-gray lava. Although the two lithologies resemble intermingled lavas, thin-section observations unequivocally show that the white rhyolite consists of broken crystals in a matrix of glassy fragments. In contrast, the red-gray rhyolite consists of unbroken crystals surrounded by flow-banded, glassy to microcrystalline groundmass. Ar-Ar dating indicates that sanidine crystals in the red-gray Peña Tank rhyolite are 22.58 ± 0.06 Ma, which is 2.6 million years younger than the 25.21 ± 0.10 Ma sanidines of the white rhyolite. The texture, mineralogy, and ages of the two rhyolite units indicates they are not intermingled lava flows, but rather that the white rhyolite originated as Amalia Tuff erupted from the Latir caldera at 25.39 ± 0.04 Ma (Zimmerer and McIntosh, in review). The slight discrepancy in sanidine age between Amalia Tuff sanidine and the Peña Tank white rhyolite may reflect slight ^{40}Ar loss related to reheating by the red-gray rhyolite. The unusual association of rhyolite lava containing bodies of older, non-welded tuff may have formed when Peña Tank Rhyolite lava erupted beneath a subaerial sheet of non-welded Amalia Tuff, incorporating large blocks of the ignimbrite. Fluidization of damp, non-lithified tuff allowed lava fragments to be mixed into the tuff and wispy tendrils of the tuff to penetrate the lava.

INTRODUCTION

Geologic Setting

The Peña Tank Rhyolite (new name) is one of the few exposed extrusive rocks recording early Miocene volcanism in the southern San Luis Basin. The Peña Tank Rhyolite is located 40-48 km west-northwest of Taos, on the western flank of the half-graben that forms the San Luis Basin (Fig. 1). This half-graben subsided during the late Oligocene through Quaternary, concomitant with Rio Grande rift extension (Lipman and Mehnert, 1979; Brister and Griggs, 1994; Chapin and Cather, 1994; Miggins et al., 2002; Bauer and Kelson, 2004; Kelson et al., 2004). The San Luis Basin has been a site of significant volcanism through much of the latter half of the Cenozoic, beginning on the west rift flank with the 33 Ma Bonanza Caldera and the 29-28 Ma Platoro Caldera complex, continuing on the east rift flank with the Latir volcanic field at 28-23 Ma, and eventually ending with voluminous Servilleta basaltic flows at 3-5 Ma (McIntosh and Chapin, 2004; Lipman et al., 1986; Zimmerer and McIntosh, in review; Chapin et al., 2004). Within this time frame, there is evidence for <22.7 Ma dacitic volcanism at Brushy Mountain and Timber Mountain, located 37 km northwest of Taos (Zimmerer and McIntosh, in review; Lipman et al., 1986; Thompson et al., 1986). Miocene volcanic centers west-northwest of Taos, which may coincide with the source of the Peña Tank Rhyolite (Fig. 1), were interpreted by Ingersoll et al. (1990) based on sedimentologic study of the Santa Fe Group. In the Peña Tank area, emplacement of the 28.28 ± 0.07 Ma Las Tablas tuff and the 25.39 ± 0.04 Ma Amalia Tuff prededed local rhyolite lava volcanism and the Peña Tank Rhyolite (Lipman et al., 1986; Zimmerer and McIntosh, 2011; Zimmerer and McIntosh, in review).

Strata overlying and underlying the Peña Tank Rhyolite include volcaniclastic units, a fine-grained, non-volcaniclastic sandstone, and basalt flows (Fig. 2; Koning et al., 2007; Aby, 2008; Aby et al., 2010). The Peña Tank Rhyolite generally overlies, or is inset against, sandy conglomerate and gravelly sandstone of the Cordito Member of the Los Pinos Formation. Pebbles, cobbles, and boulders of the Cordito Member are composed of various rhyolites, minor dacites, and minor ash-flow tuff, including the Amalia Tuff (1-2% of the gravel fraction). Cordito Member sandstone is commonly tuffaceous and contains abundant sanidine grains. Ages of some clasts from the Cordito Member are ~25 Ma (Zimmerer and McIntosh, in review). The Cordito Member overlies tan, clayey-silty very fine- to fine-grained sand that is locally interbedded with gravels (Tanque unit; Koning et al., 2011a). This fine-grained unit overlies Jarita Basalt. These basanitic flows range from 20 to 150 m in thickness and those in the vicinity of the study area have returned ages of 24.6 ± 0.7 Ma (K/Ar), 24.92 ± 0.34 Ma (^{40}Ar/^{39}Ar), and an anomalously low ^{40}Ar/^{39}Ar age of 22.72 ± 0.53 Ma (Baldridge et al., 1980; Guidebook data repository). Overlying the Peña Tank Rhyolite, and locally interbedded with it (e.g., near Petaca Mill) are volcaniclastic sandy pebbles and cobbles of the Duranes Member of the Tesuque Formation (Koning et al., 2011b). Duranes Member gravel is composed mostly of dacite and andesite (Ekas et al., 1984; Koning et al., 2011b).

A short, northwest-trending paleovalley is evident along Cañada del Abrevadero, based on inset relations of the Peña Tank Rhyolite and underlying Los Pinos Formation with Proterozoic bedrock (Fig. 3). This paleovalley was eroded in a north-south ridge composed of Proterozoic bedrock. The head of the 3-4 km-

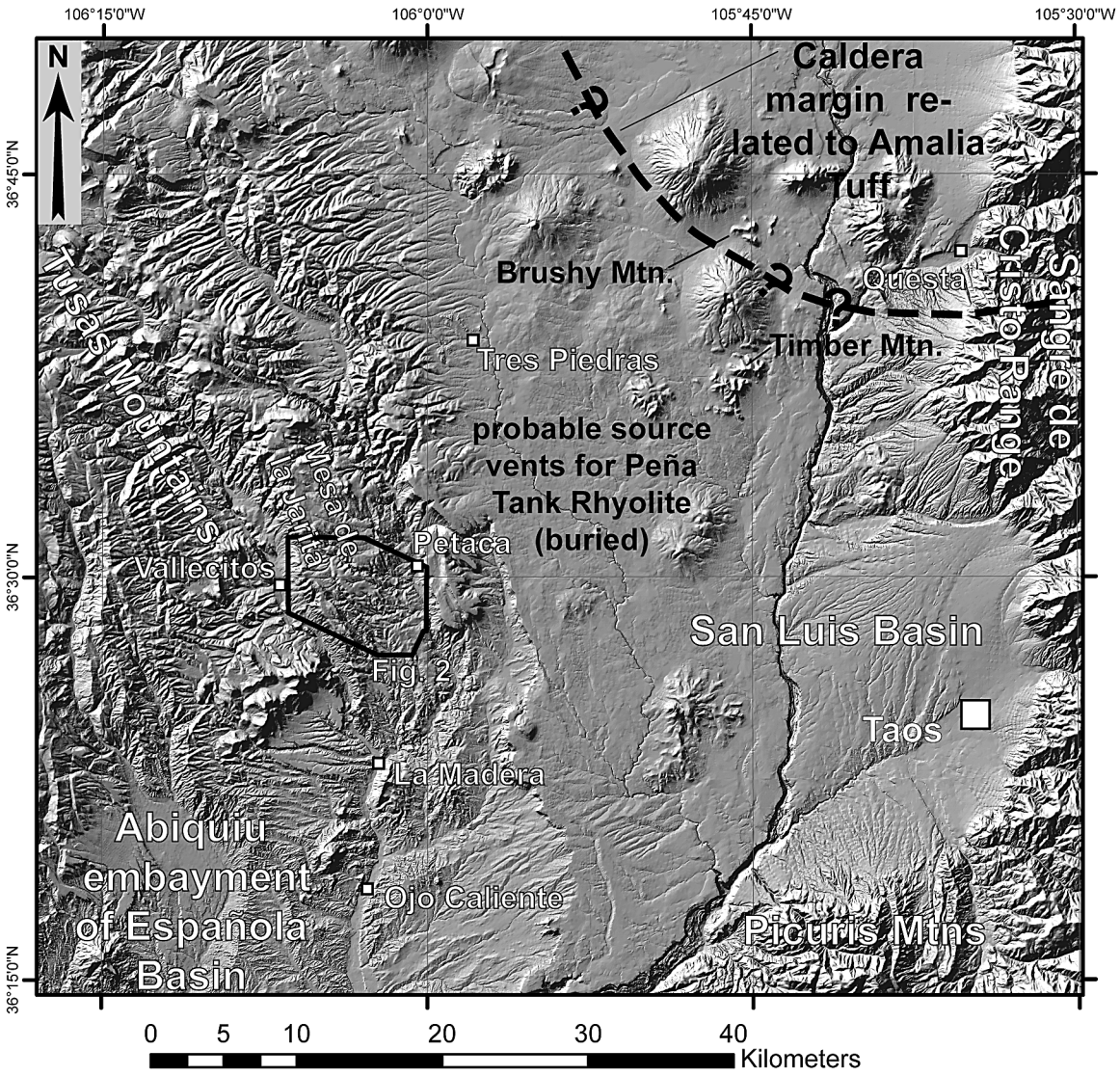

FIGURE 1. Location map showing the San Luis and Española Basins, the inferred source of the Peña Tank Rhyolite, and various towns and cities. The location of the study area (Figure 3) is depicted by the black polygon.

long paleovalley was located about 2 km upstream of the mouth of the modern canyon. A former river depositing the Los Pinos Formation flowed northwest through this paleovalley, based on paleocurrent data (Koning et al., 2007; Aby et al., 2010). Within the Cañada del Abrevadero paleovalley, the Peña Tank Rhyolite is commonly inset against the Cordito Member along a buttress unconformity. Evidently, the river incised after deposition of the Cordito Member and the resulting inner paleovalley was filled by the Peña Tank Rhyolite.

Peña Tank Rhyolite

We propose the new name "Peña Tank Rhyolite" for the rhyolitic flow complex exposed west and south of the village of Petaca (Fig. 3). We designate the type locale on Mesa de la Jarita, 800 m northwest of Peña tank (Figs. 1, 4). Peña Tank is located in the headwaters of Cañada de los Apaches, 5.8 km west of Petaca and 3.6 km northwest of the town of Vallecitos (Figs. 1, 3, 4).

The exposed area of the Peña Tank Rhyolite west of the Rio Tusas is ~25 km^2 (Fig. 3), but the unit very likely extends eastward in the subsurface. Its thickness is generally 5-15 m although it reaches a maximum thickness of 55 m in the Abrevadero paleovalley. The aspect ratio (thickness/lateral extent) of the flow is unusually low for a rhyolite lava. This rhyolite is locally flow brecciated (Fig. 5) and locally flow-banded. For most of its mapped area, the Peña Tank Rhyolite flow complex appears to represent one brief extrusive event. No oxidized, intraflow rubble zones, paleosols, or epiclastic sediments were observed within the flow complex. An exception to this general observation is found 3 km south of Petaca, near the abandoned Petaca mill, where three distinct flows separated by volcaniclastic units appear to be present. Based on geologic mapping, the lower flow of the Peña Tank

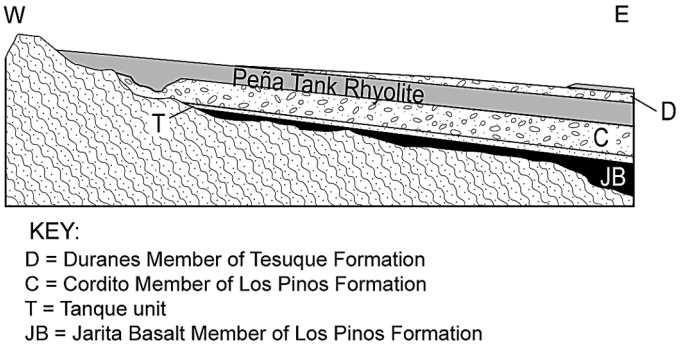

FIGURE 2. Schematic cross-section diagram illustrating stratigraphic relations southwest of Petaca, New Mexico.

Rhyolite appears to have been the most extensive, whereas higher flows were restricted to the Petaca mill area.

White rhyolitic pods in red-gray rhyolite lava

One of the distinguishing characteristics of the Peña Tank Rhyolite is the presence of white, rhyolitic pods or inclusions within a more voluminous, red-gray rhyolitic lava flow (Fig. 6). Colors of the red-gray rhyolite range from red, light purple, reddish brown, reddish gray to gray. The phenocrystic minerals include: 5-30% sanidine and other alkalic feldspars, 0.5-10% hornblende and biotite, and 0 to 1% quartz (mostly 1% and locally up to 7%). Sanidine and other alkalic feldspars are typically the largest phenocrysts (0.5-10 mm, up to 10-30 mm). Quartz phenocrysts are 0.5-7 mm (mostly 0.5-2.0 mm), hornblende ranges from 0.2-9 mm (mostly <5 mm), and biotite is 0.2- 4 mm-long.

The white rhyolitic pods within the red-gray rhyolite lava are referred to as the white subunit in the First-Day Road Log but simply as the 'white rhyolite' in this paper. They are generally tabular in shape and range in size from a few meters to as large as 400 m in maximum dimension. Colors of unweathered surfaces

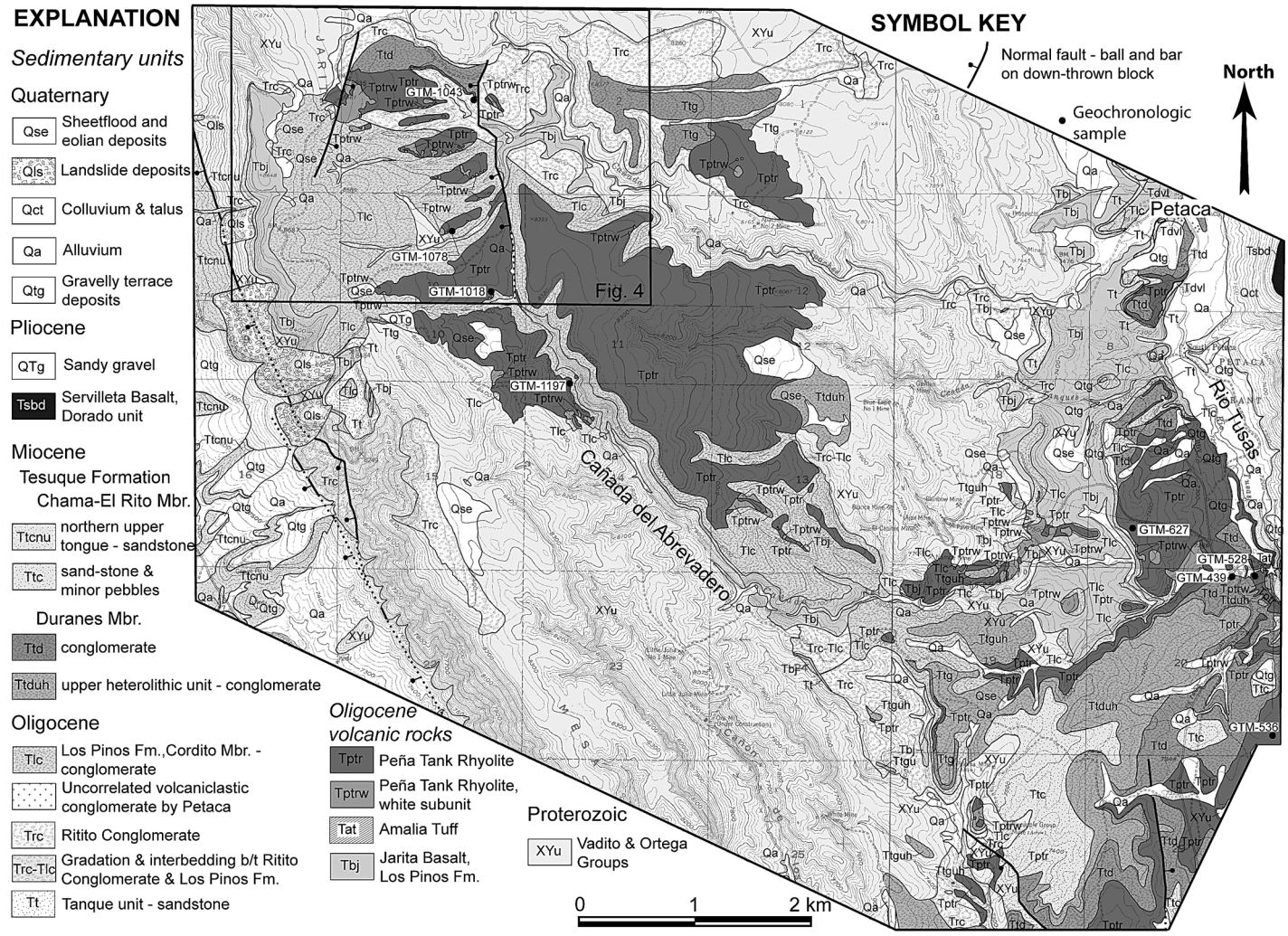

FIGURE 3. Geologic map showing the Peña Tank Rhyolite flow complex in the southeastern Tusas Mountains. Star symbol along eastern map margin denotes location of the Petaca pegmatite mill. Rectangle in upper left outlines the location of the Figure 4 geologic map. Map slightly modified from Koning et al. (2007).

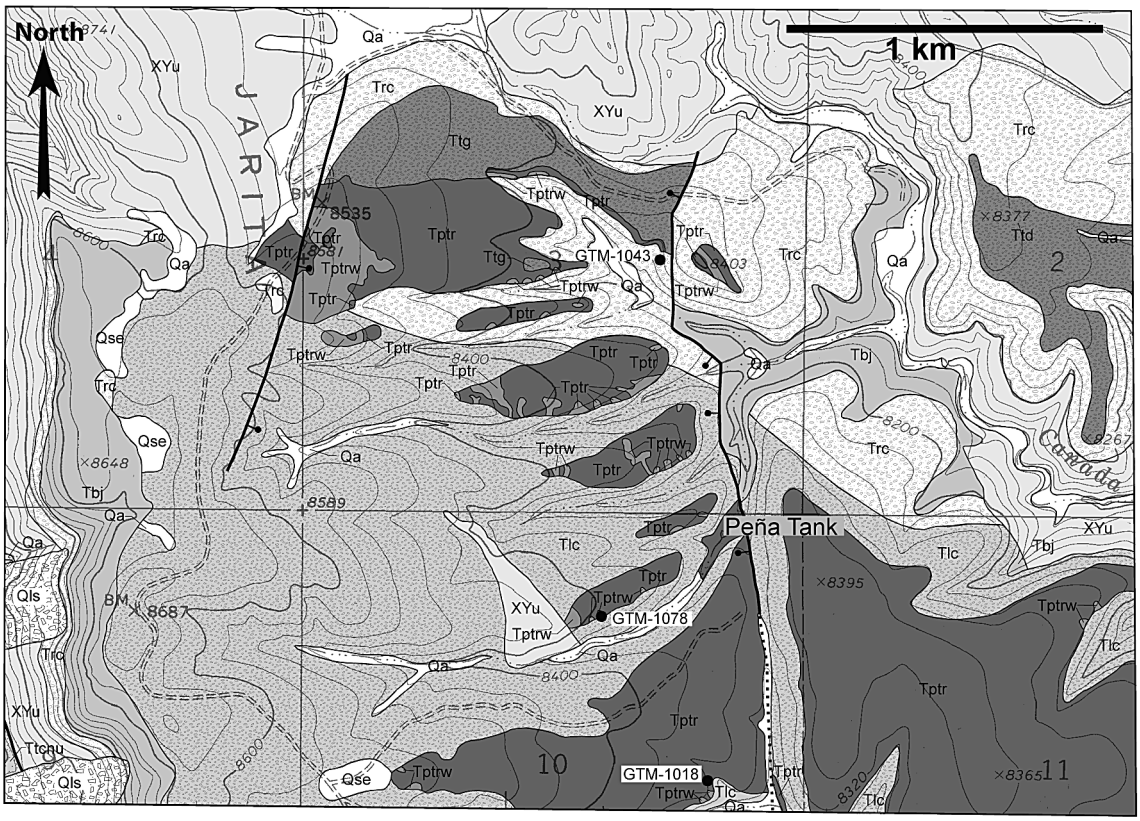

FIGURE 4. Geologic map illustrating the Peña Tank Rhyolite near Peña Tank. The Peña Tank, actually a dirt-floored reservoir, is located 5.8 km west of Petaca and 3.6 km northwest of the town of Vallecitos. Map slightly modified from Aby et al. (2010).

range from light gray to tannish white to chalky white, and outcrops weather to a white color. The light gray and tannish white rhyolite are fresh, whereas chalky white rhyolite may be related to vapor-phase alteration. Generally, the chalky white rhyolite appears near the outer margins of the pods. The white subunit contains phenocrysts in aphanitic groundmass. The phenocrysts include 10-25% smoky quartz phenocrysts (0.2-2.0 mm long), 0.5-8% chatoyant sanidine (0.5-2.0 mm long), and trace biotite. This rock contains trace to 0.5%, locally as much as 8%, xenoliths of red-gray rhyolite lava (up to 13 mm long) and rhyodacite lava (1-28 mm long). Outcrop relations indicate that the margins of the white rhyolite were more fluid than the red-gray Peña Tank lava during eruption and emplacement. Pebble-size xenoliths of the red-gray rhyolite are common within the white rhyolite, and veins of the white rhyolite penetrate into the red-gray lava (Fig. 7).

HYPOTHESES

A variety of hypotheses were considered in the field to explain the genesis of the white rhyolite in the red-gray lavas of the Peña Tank rhyolite. One possibility was that the white rhyolite was intruded into the red-gray lava. A second possibility was that two magmas were erupted simultaneously, probably from a zoned magma chamber, and commingled during the eruption. A third possibility was that the white pods were large xenoliths incorporated into the red-gray lava at the time of eruption, and that the fluidal textures reflect partial melting of the white xenoliths by the host red-gray lava, which we presumed to be more mafic and hotter. According to the latter hypothesis, heat from the red-gray lavas partially melted the margins of the xenolithic bodies but not the cores, allowing penetrative relations of the white subunit and xenoliths of the red-gray lava in the outer margins of the white subunit. Another study (Wiebe, 1980) has noted fluidal textures in comingled magmas or magmas with partially melted xenoliths, similar to the fluidal shapes and penetrative veins along the margins of the white rhyolite.

METHODS

In order to test the various hypotheses for the origin of the white rhyolitic pods in the red-gray Peña Tank Rhyolite, we employed a number of methods, including geologic mapping and outcrop observations, chemical analyses, thin-section examinations, and $^{40}Ar/^{39}Ar$ dating. We first mapped the spatial distribution, abundance, and relative location of the white rhyolitic pods in the red-gray lava. We collected a representative suite of samples from both the white rhyolite and the red-gray lava, including interiors and marginal facies of the white subunit. Three samples of both lithologies were submitted for whole-rock elemental analyses at the Washington State University x-ray florescence facility (Appendix 1). Eight representative samples, including samples

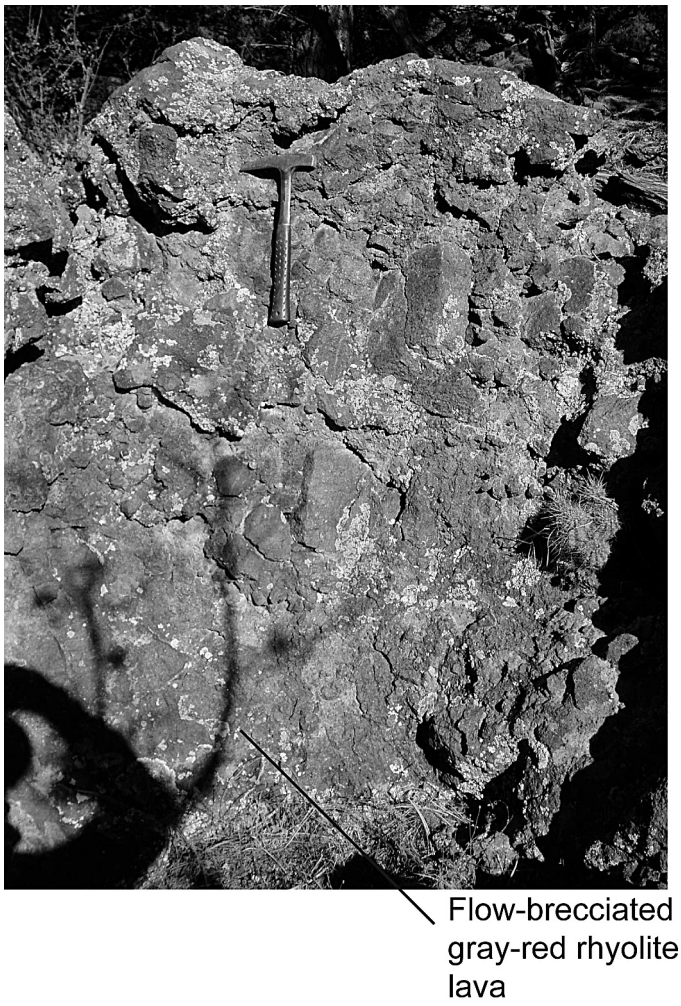

FIGURE 5. Photograph of flow-brecciated red-gray lava of the Peña Tank Rhyolite.

that crossed the contacts between lithologies, were thin-sectioned and examined by petrographic microscope. Finally, sanidine separates were prepared from five representative samples of both lithologies, including two samples of red-gray lava and three samples of cores and veins of the white subunit. Biotite separates were prepared from two other samples of red-gray lava. All separates were irradiated along with monitor minerals of known age, then dated using single-crystal laser-fusion methods (sanidine) or resistance-furnace incremental heating (biotites) on the MAP 215-50 mass spectrometer at the New Mexico Geochronology Research Lab in Socorro, New Mexico. Details of sample preparation and analysis, together with complete tables of analytical data, are presented in the Guidebook data repository.

RESULTS

Field Mapping

The size, shape, and distribution of the white rhyolite were assessed during geologic mapping of the study area (Figs. 3-4).

FIGURE 6. Photograph of red-gray lava overlying the white rhyolite. The white line is drawn at the contact between the two units.

Geologic mapping was conducted between 2006 and 2010 at a scale of 1:12000 as part of the STATEMAP component of the National Geologic National Cooperative Geologic Mapping Program (Koning et al., 2007; Aby et al., 2010). The white rhyolitic pods are irregular in shape and range in size from ~3 m to ~400 m. Most of these rhyolitic bodies are 3-150 m in length. Pods that are less than 50 m are commonly found at the bottom of the flow (Fig. 4). In regards to their distribution, the white rhyolitic pods are most common on the western and southern extents of the Peña Tank Rhyolite and least common to the northeast (Figs. 3, 4). No internal contacts were observed within the white rhyolitic pods. Based on the distribution of the Peña Tank Rhyolite and underlying Los Pinos Formation strata, it is interpreted that the red-gray rhyolite flowed from east to west and passed through a ridge of Proterozoic bedrock via the aforementioned northwest-trending paleovalley along Cañada del Abrevadero.

Geochemical Analysis

Major element analyses (Fig. 8, Appendix 1) indicate that both the red-gray lava (two samples) and the white subunit (one sample) are rhyolitic in composition. Analytical totals range from 95% to 98%, probably reflecting some hydration of volcanic glass. After normalizing the totals to 100%, the gray red lava is compositionally a low-to-medium silica rhyolite; analyses of two samples average 74% SiO_2. The analyzed white pod appears to be a high-silica rhyolite. The SiO_2 value of 79% suggests modest post-emplacement elevation of silica, either by vapor phase alteration or later silicification.

$^{40}Ar/^{39}Ar$ Analysis

$^{40}Ar/^{39}Ar$ analysis of sanidine separates indicate that the eruption ages of the red-gray lava and the white pods differ systematically by 2.6 million years (Fig. 9, Table 1, Appendix 2). Ages of individual sanidine crystals from two samples of red-gray lava (samples GTM-528-djk and GTM-1018 in Fig. 10) are unimod-

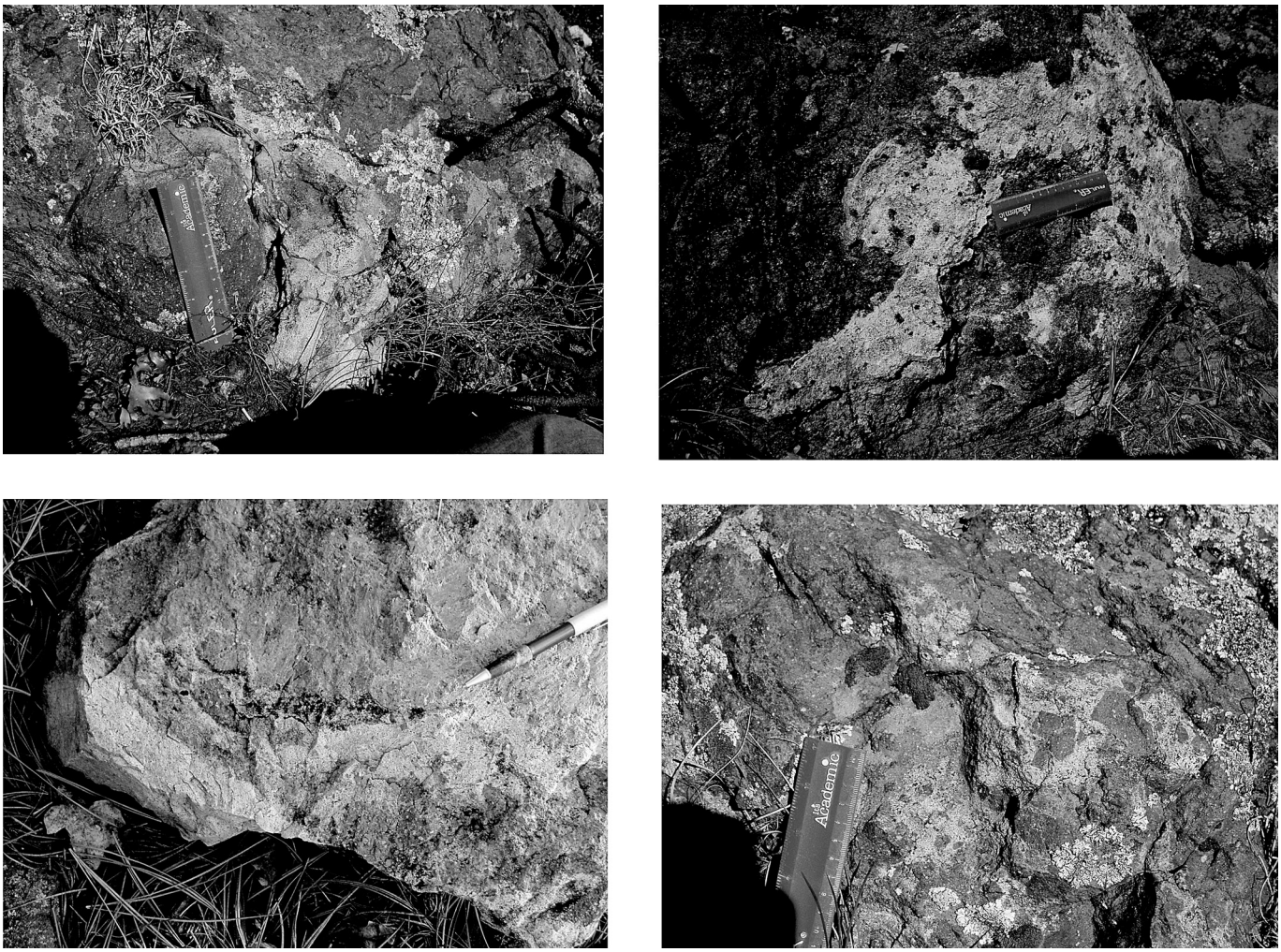

FIGURE 7. Four photographs illustrating veining of the white rhyolite into the red-gray lava (top two photographs) and xenoliths of the red-gray lava in the white rhyolite (lower two photographs). In lower left photograph, the pencil points to the contact between the two units.

ally distributed and yield statistically indistinguishable weighted mean ages of 22.62 ± 0.08 Ma and 22.53 ± 0.06 Ma (all ages relative to Fish Canyon Tuff sanidine at 28.201 Ma (Kuiper et al., 2008); all errors quoted at ± 2 sigma). Incrementally heated biotite separates from two other samples of red-gray lava (Fig. 11) yielded flat age spectra with slightly older plateau ages of 23.02 ± 0.07 Ma and 23.21 ± 0.09 Ma. Because volcanic biotites are notorious for yielding apparent ages as much 500 ka older than eruption ages determined by other means (Bachmann et al., 2010; Hora et al., 2010), the most accurate eruption age determination for the red-gray lava is the weighted mean of the two sanidine ages, 22.58 ± 0.06 Ma.

Sanidine separates from two of the three samples of the white subunit (Fig. 10) yielded unimodal distributions of age and weighted mean ages of 25.21 ± 0.07 Ma (sample GTM-536) and 25.04 ± 0.24 Ma (sample GTM-439). The low precision of the latter age determination is due to small crystal size and possible slight alteration of the sanidine. Sanidine crystals from a sample of the margin of a white pod (sample GTM-1043) yield a spread of single crystals from 22.5 to 25.9 Ma. The ages of seven crystals from this sample are tightly grouped, yielding a weighted mean age of 25.33 ± 0.08 Ma. The weighted mean of the three ages from the three samples of the white subunit is 25.21 ± 0.10 Ma.

Thin section observations

Thin sections of the red-gray lava and the white lava are petrogaphically very different. The red-gray unit appears to be a typical rhyolite lava (Fig. 12a). Phenocrysts tend to be unbroken and are contained in a matrix of microphenocryst-rich glassy groundmass. Microphenocrysts in the matrix are dominantly 20 to 150 μm feldspars showing strong alignment typical of flow foliations in high viscosity silicic melts.

In contrast to the red-gray lavas, the majority of phenocrysts in the white rhyolite are angular fragments characteristic of

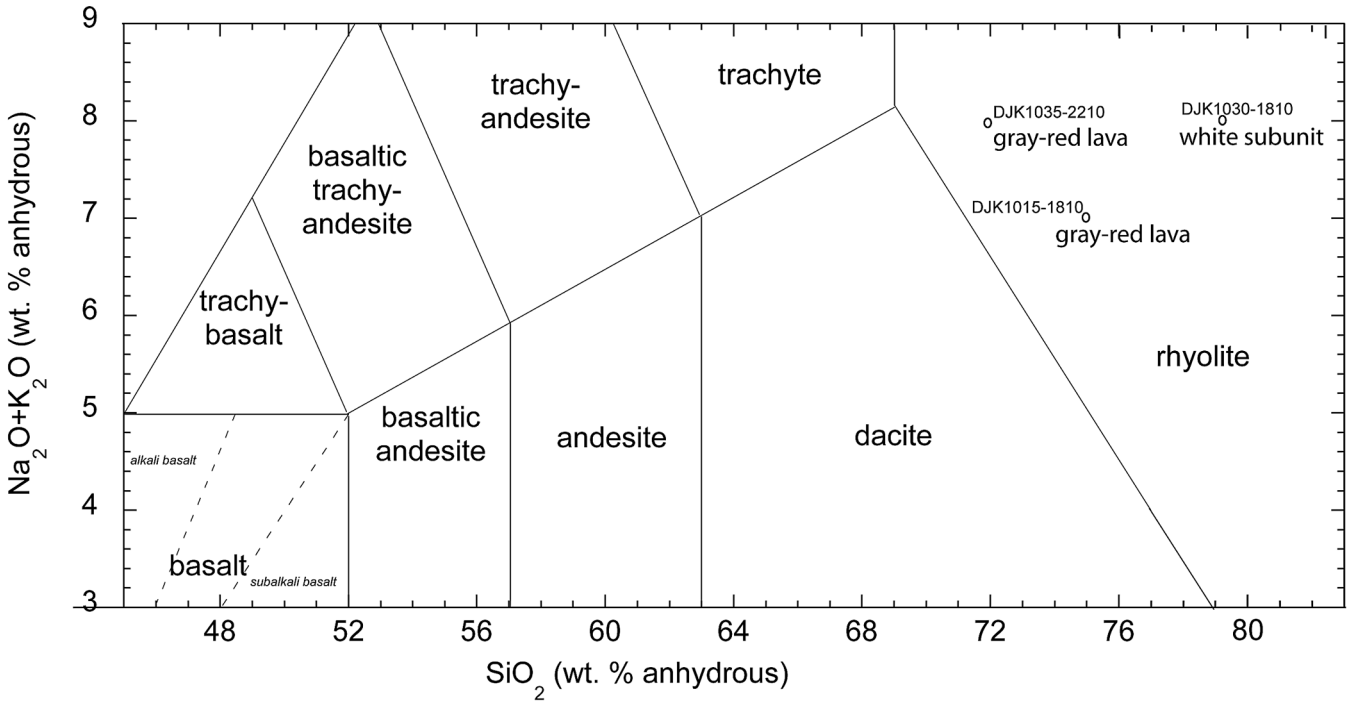

FIGURE 8. Composition of the Peña Tank Rhyolite illustrated on a LeBas diagram.

ignimbrites (Fig. 12b). Fragmentation of phenocrysts in ignimbrites commonly occurs due to explosive depressurization of melt inclusions within the crystals (Best and Christiansen, 1997). The matrix of the white rhyolite samples (Fig. 12b) also differs strongly from that of the red-gray lava. It consists of finely comminuted glass fragments, typically 20-200 µm. Most of the fragments appear to be equidimensional and angular, but some exhibit distinctive shard morphologies typical of silicic pyroclastic rocks. The matrix of the white rhyolite lacks microphenocrysts and shows no flow alignment, unlike the red-gray lava.

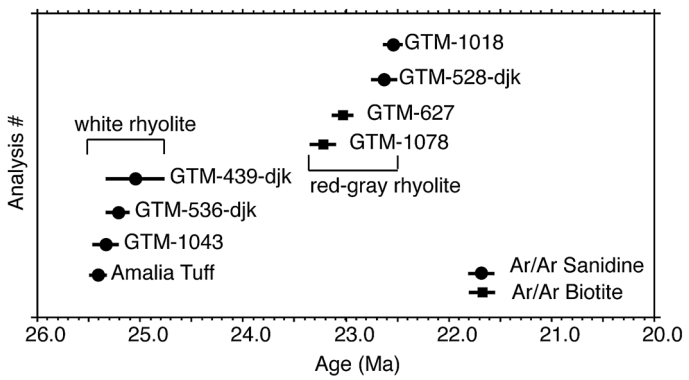

FIGURE 9. Summary of $^{40}Ar/^{39}Ar$ dating results for the Peña Tank Rhyolite.

DISCUSSION

Although initial field observations suggested that the red-gray lava and white rhyolite might represent two co-mingled lavas, thin section observations and $^{40}Ar/^{39}Ar$ dating indicate that the white pods are in fact bodies of non-welded, pyroclastic rhyolite tuff, probably ignimbrite, that were emplaced 2.6 million years prior to being incorporated in the red-gray rhyolite lava. Fluidal textures at the margins of the white subunit, thought to indicate melting based solely on outcrop observations, in fact represent fluidization and remobilization of fragmental material. Christiansen and Lipman (1966) describe similar fluidized structures and remobilization of fragmental material in fused bedded tuffs beneath a rhyolite lava in southern Nevada.

The age (25.21 ± 0.10 Ma) and phenocryst content of the white rhyolite strongly suggest that they originated as non-welded Amalia tuff. Amalia Tuff was erupted from the Questa caldera at 25.39± 0.04 Ma (Zimmerer and McIntosh, in review). The age of sanidines from the white subunit is slightly but distinguishably (at ± 2 sigma) younger that the age Amalia Tuff. This small discrepancy may reflect minor loss of ^{40}Ar caused by reheating of the white tuff clasts by the enclosing red-gray rhyolite lava. The eastern margin of the Questa caldera is exposed along the eastern flank of the Rio Grande rift about 45 km east of the outcrops of the Peña Tank Rhyolite. The western margin of the Questa caldera is not exposed and is probably buried beneath the Rio Grande rift (Fig. 1). Outcrops of non-welded and welded Amalia

TABLE 1. $^{40}Ar/^{39}Ar$ radioisotopic age data for the Peña Tank Rhyolite.

Sample	UTM coordinates (m) Zone13, NAD 27	General location	Description	Lab sample number	Mineral	analysis	n	Age ± 2σ (Ma)
			Red-gray lava					
GTM-528-djk	410,195 E 4,037,390 N	150 m southwest of the Petaca mill site, on the south slope of mouth of Canada del Abrevadero.	Gray (N5-6/), porphyritic dacite with 10% plagioclase and sanidine phenocrysts up to 10 mm long. Phenocrysts also include 1% quartz (up to 3 mm) and 3-5% hornblende together with minor biotite (<2 mm). Flow lies below a tongue of volcaniclastic gravel with black, dacitic(?) clasts.	57802	Sanidine	SCLF	15	22.62 ± 0.08
GTM-627-djk	409,139 E 4,037,803 N	60 m south of the Rainbow mine rd, 700 m west of where this road intersects State Highway 519.	2 m-thick, pink, plagioclase-biotite-hornblende-quartz volcanic flow that directly overlies the Cordito Member of the Los Pinos Formation	57852	biotite	FSH	12	23.02 ± 0.07
GTM-1018	403,617 E 4,039,845 N	Eastern Mesa de la Jarita, 5.9 km west of Petaca	Large body of gray lava with megacrystic sanidine within the Pena Tank rhyolite flow complex. Sample is gray with ~15% sanidine crystals (2 -30 mm long), 10% hornblende up to 3 mm-long; trace quartz phenos.	59091	Sanidine	SCLF	11	22.53 ± 0.06
GTM-1078	403,281 E 4,040,366 N	Mesa de la Jarita, 440 m southwest of Pena Tank.	Pena Tank flows overlie the Cordito Mbr. Sample is a pinkish to light purple dacite; flow-banded, with 12-15% Kspar phenocrysts (1-4 mm) and 12% hornblende and minor biotite (0.5-3.0 m in length).	59109	Biotite	FSH	8	23.26 ± 0.10
			White subunit					
GTM-439-djk	409,997 E 4,037,386 N	90 m west of State Road 519, near mouth of Canada del Abrevadero on its south slope. NW La Madera 7.5-minute quadrangle.	White rhyolite, with 20-25% quartz phenocrysts (brownish gray color and 0.2-2.0 mm-long). The rest of the rock is aphanetic groundmass with 0.5% lithic fragments of silicic volcanic rocks (and quartzite?) up to 6 mm-long. Sampled from interior of unit.	57800	Sanidine	SCLF	14	25.04 ± 0.24
GTM-536-djk	410,347 E 4,036,022 N	4.5 km south of the town of Petaca and 700 m east of Highway 519.	White-colored rhyolite, with common quartz phenocrysts and very minor chatoyant sanidine. White subunit is clearly in middle of a gray-red lava flow.	57801	Sanidine	SCLF	14	25.21 ± 0.07
GTM-1043	403,467 E 4,041,497 N	Headwaters of Canada de los Apaches, 6.1 km WNW of Petaca, NM	The Pena Tank complex is 6 m-thick and overlies Rito Conglomerate. Flow is overlain by dacitic-rhyolitic gravel. Sample is white to tannish white and contains a phenocryst assemblage of: ~20% smoky quartz <2 mm-long, ~5% sanidine, and trace biotite.	59090	Sanidine	SCLF	7	25.33 ± 0.08

Notes: Analyses performed at the New Mexico Geochronology Research Laboratory. Ages calculated relative to FC-2 Fish Canyon Tuff sanidine interlaboratory standard (28.201 Ma, Kuiper et al, 2008). SCLF = single-crystal laser fusion; FSH = furnace step-heat; Mbr = Member; Fm = Formation, n = number of analyses used in weighted mean age (SCLF) or number of steps in age plateau (FSH).

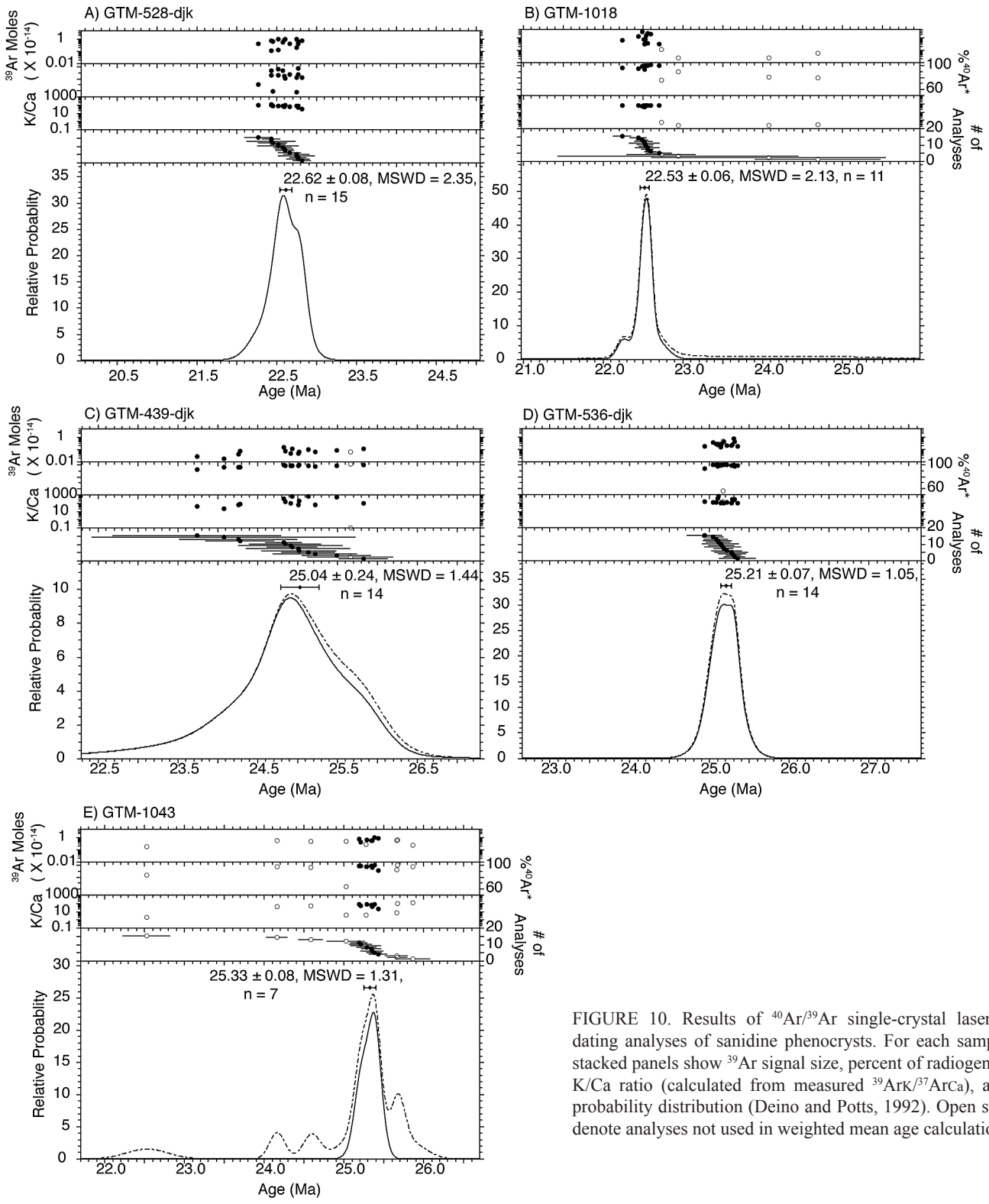

FIGURE 10. Results of $^{40}Ar/^{39}Ar$ single-crystal laser-fusion dating analyses of sanidine phenocrysts. For each sample, the stacked panels show ^{39}Ar signal size, percent of radiogenic ^{40}Ar, K/Ca ratio (calculated from measured $^{39}Ar_K/^{37}Ar_{Ca}$), and age probability distribution (Deino and Potts, 1992). Open symbols denote analyses not used in weighted mean age calculations.

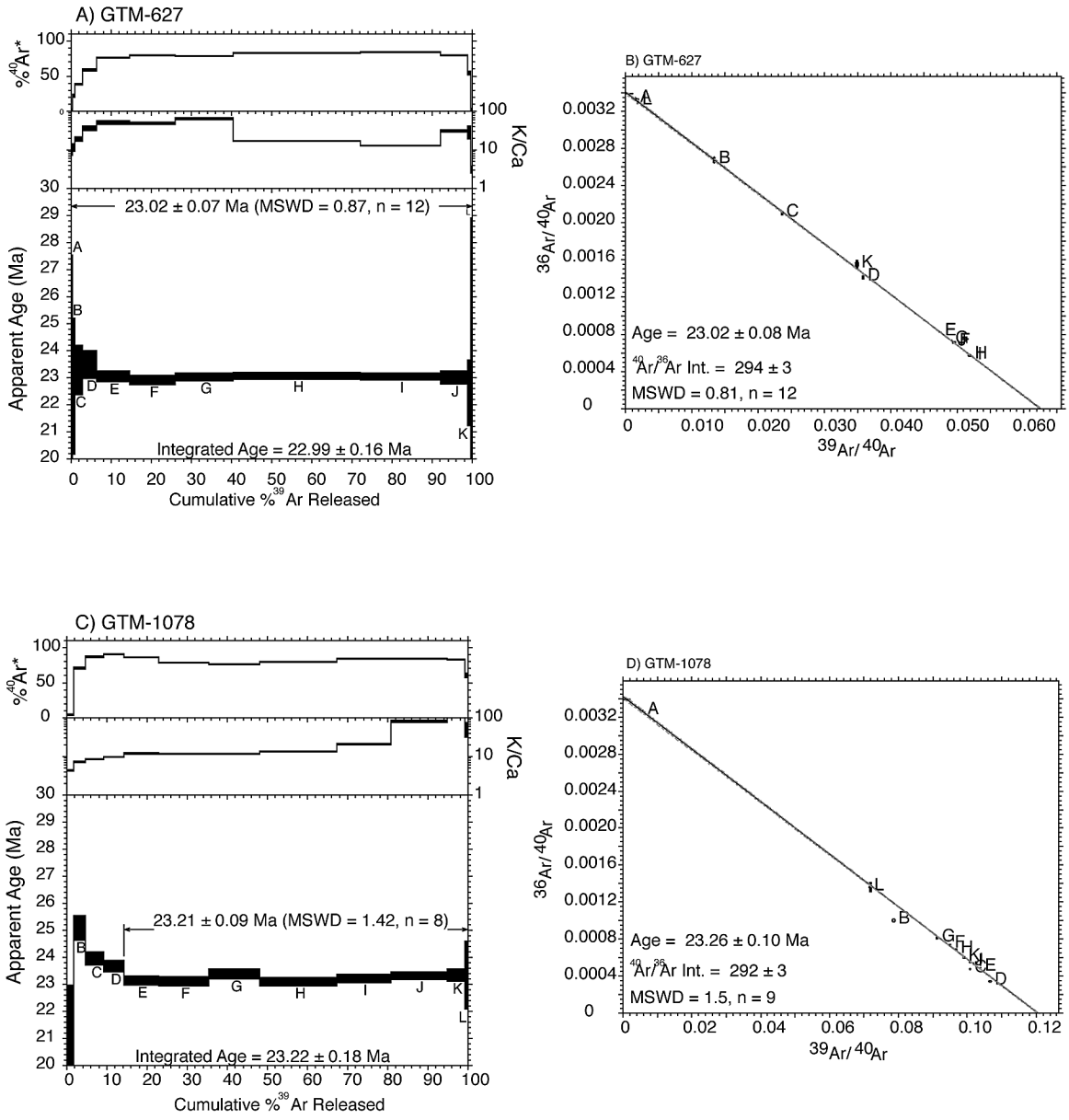

FIGURE 11. Results of $^{40}Ar/^{39}Ar$ resistance-furnace incremental-heating dating analyses of biotite separates. For each sample, the stacked panels on the left show percent of radiogenic ^{40}Ar, K/Ca ratio (calculated from measured $^{39}Ar_K/^{37}Ar_{Ca}$), age spectrum, and plateau age. Results are also presented on inverse isochron diagrams.

Tuff are exposed in the vicinity of the Peña Tank Rhyolite, such as the welded tuff at Petaca mill and the non-welded tuff 13 km to the north (Stop 1 of Day 2 of the Road Log).

We interpret the white rhyolitic pods within the red-gray Peña Tank Rhyolite lava to be bodies of non-welded Amalia Tuff that were incorporated within the rhyolite lava during its eruption and emplacement. The margins of the bodies of tuff were locally fluidized during this process, allowing clasts of lava to be incorporated into the tuff and veins of tuff to penetrate the rhyolite lava. Fluidization probably occurred when moisture in the tuff was heated and flashed to steam as the surrounding lava heated the tuff. We do not know the mechanism by which blocks of tuff were incorporated into the lava, but suggest that the blocks are far too large to have been erupted from a vent. Instead, we speculate that the lava may have initially been emplaced as a sill-like body beneath a low-density layer of non-welded Amalia Tuff exposed at the earth's surface. Inflation of the lava broke the overlying tuff into blocks that were transported laterally by flow of the lava, resulting in tuff blocks concentrated near the margin of the flow. As the margins of the tuff blocks heated up, they were locally fluidized to produce the intriguing textures now seen in the Peña Tank Rhyolite flow complex.

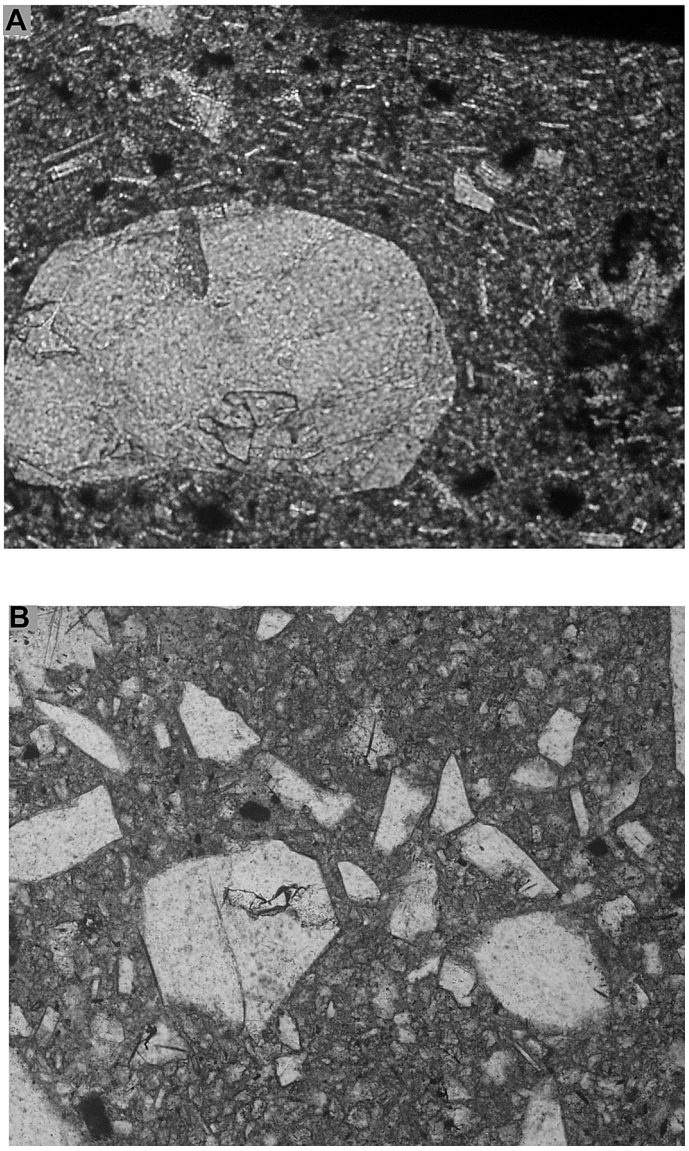

FIGURE 12. Thin section photomicrographs of the Peña Tank Rhyolite: a) red-gray lava, and b) pod of white rhyolite.

ACKNOWLEDGMENTS

The Peña Tank Rhyolite was studied during mapping of the La Madera and Las Tablas 7.5-minute quadrangles. This mapping was funded by the STATEMAP component of the National Cooperative Geologic Mapping Program. We appreciate input from Charles Chapin and useful reviews by David Broxton and Shari Kelley.

REFERENCES

Aby, S.B., 2008, Geologic map of the Servilleta Plaza Quadrangle, Taos and Rio Arriba Counties, New Mexico: New Mexico Bureau of Geology and Mineral Resources, Open-file Geologic Map OF-GM-182, scale 1:24,000.

Aby, S., Karlstrom, K., Koning, D., and Kempter, K., 2010, Preliminary geologic map of the Las Tablas quadrangle, Rio Arriba County, New Mexico: New Mexico Bureau of Geology and Mineral Resources, Open-file Geologic Map 200, 1:12,000.

Bachmann, O., Schoene, B., Schnyder, C., and Spikings, R., 2010, The $^{40}Ar/^{39}Ar$ and U/Pb dating of young rhyolites in the Kos-Nisyros volcanic complex, Eastern Aegean Arc, Greece: Age discordance due to excess ^{40}Ar in biotite: Geochemistry Geophysics Geosystems, vol. 11 p. 1-14.

Baldridge, W.S., Damon, P.E., Shafiqullah, M., and Bridwell, R.J., 1980, Evolution of the central Rio Grande rift, New Mexico - new Potassium-Argon ages: Earth and Planetary Science Letters, v. 51, p. 309-321.

Bauer, P.W., and Kelson, K.I., 2004, Cenozoic structural development of the Taos area, New Mexico: N.M. Geological Society, 55th Field Conference Guidebook, p. 129-146.

Best, M.G. and Christiansen. E.H., 1997, Origin of broken phenocrysts in ash flow tuffs: Geological Society of America Bulletin, v. 109, p. 63-73.

Brister, B.S., and Gries, R.R., 1994, Tertiary stratigraphy and tectonic development of the Alamosa basin (northern San Luis basin), Rio Grande rift, south-central Colorado: Geological Society of America, Special Paper 291, p. 39-58.

Chapin, C.E., and Cather, S.M., 1994, Tectonic setting of the axial basins of the northern and central Rio Grande rift: Geological Society of America, Special Paper 291, p. 5-26.

Chapin, C.E., Wilks, M., and McIntosh, W.C., 2004, Space-time patterns of Late Cretaceous to Present magmatism in New Mexico-Comparison with Andean volcanism And potential for future volcanism: New Mexico Bureau of Geology and Mineral Resources Bulletin, v. 160, p. 13-40.

Christiansen. R.L. and Lipman, P.W., 1966, Emplacement and Thermal History of a Rhyolite Lava Flow near Fortymile Canyon, Southern Nevada: Geological Society of America Bulletin, v. 77, p. 671-684.

Deino, A. and Potts, R., 1992. Age-probability spectra for examination of single-crystal $^{40}Ar/^{39}Ar$ dating results: examples from Olorgesailie, Southern Kenya Rift. Quaternary International, v. 13/14, 47-53.

Ekas, L.M., Ingersoll, R.V., Baldridge, W.S., and Shafiqullah, M., 1984, The Chama-El Rito Member of the Tesuque Formation, Española Basin, New Mexico: New Mexico Geological Society Guidebook, 35th Field Conference, Guidebook, p. 137-143.

Hora, J.M., Singer, B.S., Jicha B.R., Beard B.L., Johnson C.M., de Silva, S. and Salibury, M., 2010, Volcanic biotite-sanidine $^{40}Ar/^{39}Ar$ age discordances reflect Ar partitioning and pre-eruption closure in biotite; Geology, Vol. 38, pp. 923-926.

Kelson, K.I., Bauer, P.W., Unruh, J.R., and Bott, J.D.J., 2004, Late Quaternary characteristics of the northern Embudo fault, Taos County, New Mexico: N.M. Geological Society, 55th Field Conference Guidebook, p. 147-157.

Koning, D.J., Karlstrom, K., Salem, A., and Lombardi, C., 2007, Preliminary geologic map of the La Madera quadrangle, Rio Arriba County, New Mexico: New Mexico Bureau of Geology and Mineral Resources, Open-file geologic map 141, scale of 1:12,000.

Koning, D.J., Aby, S.B., and Kempter, K.A., 2011a, Stratigraphy near South Petaca, north-central New Mexico: N.M. Geological Society, 62nd Field Conference, p. XX.

Koning, D.J., Kempter, K.A., Peters, L., McIntosh, W.C., and May, S.J., 2011b, Miocene-Oligocene volcaniclastic deposits in the northern Abiquiu embayment and southern Tusas Mountains, New Mexico: N.M. Geological Society, 62nd Field Conference, p. XX.

Kuiper, K. F., Deino, A., Hilgen, F. J., Krijgsman, W., Renne, P. R., and Wijbrans, J. R., 2008, Synchronizing rock clocks of earth history: Science, v. 320, p. 500-504.

Lipman, P.W., and Mehnert, H.H., 1975, Late Cenozoic basaltic volcanism and development of the Rio Grande depression in the southern Rocky Mountains, *in* Curtis, B.F., ed., Cenozoic history of the Southern Rocky Mountains: Geological Society of America Memoir 144, p. 119-154.

Lipman, P. W., Mehnert, H. H., Naeser, C. W., and Keller, G. R., 1986, Evolution of the Latir volcanic field, northern New Mexico, and its relation to the Rio Grande Rift, as indicated by potassium-argon and fission track dating: Journal of Geophysical Research, v. 91, p. 6329-6345.

McIntosh, W.C., and Chapin, C.E., 2004, Geochronology of the Central Colorado Volcanic Field: New Mexico Bureau of Geology and Mineral Resources Bulletin, v. 160, p. 205-238.

Miggins, D.P., Thompson, R.A., Pillmore, C.L., Snee, L.W., Stern, C.R., 2002, Extension and uplift of the northern Rio Grande rift: evidence from 40Ar/39Ar geochronology from the Sangre de Cristo Mounains, south-cen-

tral Colorado and northern New Mexico: Geological Society of America, Special Paper 362, p. 49-66.

Thompson, R. A., Dungan, M. A., and Lipman, P. W., 1986, Multiple differentiation processes in the early-rift calc-alkaline volcanics, northern Rio Grande rift, New Mexico: Journal of Geophysical Research, v. 91, p. 6046-6058.

Wiebe, R.A., 1980, Commingling of contrasted magmas in the plutonic environment: examples from the Nain anorthositic complex, Journal of Geology, v.88, p. 197-209.

Zimmerer, M.J., and McIntosh, W.C., 2011, $^{40}Ar/^{39}Ar$ dating, sanidine chemistry, and potential sources of the Las Tablas Tuff, northern New Mexico: N.M. Geological Society, 62nd Field Conference Guidebook, p. 215-222.

Zimmerer, M.J., and McIntosh, W.C., in review, The Ar/Ar geo- and thermochronology of the Latir volcanic field and the associated intrusions: Understanding caldera magmatic processes using the volcanic-plutonic relationship, submitted to Geological Society of America Bulletin,.

APPENDIX 1. Whole-rock analyses of major and trace elements

	Unnormalized Elements				Normalized Elements		
	gray-red rhyolite		white rhyolitc pod		gray-red rhyolite		white rhyolitc pod
	DJK1015 -1810	DJK1035 -2210	DJK1030 -1810		DJK1015 -1810	DJK1035 -2210	DJK1030 -1810
	Major Elements (Weight %):				Major Elements (Weight %):		
SiO2	72.57221	70.65198	75.13117	SiO2	74.989109	71.953709	79.21923923
TiO2	0.36902	0.42178	0.20672	TiO2	0.3813096	0.4295511	0.217968137
Al2O3	12.17218	13.80099	10.22887	Al2O3	12.577555	14.055267	10.78544763
FeO*	2.15308	2.45722	1.21759	FeO*	2.2247848	2.5024931	1.283842026
MnO	0.04151	0.03782	0.09124	MnO	0.0428924	0.0385168	0.09620459
MgO	0.66005	0.82644	0.1176	MgO	0.6820319	0.8416668	0.123998901
CaO	1.88909	2.06632	0.20864	CaO	1.9520031	2.104391	0.219992609
Na2O	3.44495	3.96497	3.29469	Na2O	3.5596784	4.0380227	3.473962076
K2O	3.35193	3.82463	4.32418	K2O	3.4635606	3.895097	4.559469124
P2O5	0.12299	0.13875	0.01885	P2O5	0.127086	0.1413064	0.019875674
Total	96.777	98.19088	94.83955	Total	100.00001	100.00002	100
	Trace Elements (ppm)				Trace Elements (ppm)		
Ni	9.3	10.6	0	NiO	11.834492	13.488775	0
Cr	13.4	15.5	3.6	Cr2O3	19.585091	22.654396	5.261666282
Sc	4.5	4.8	2.3	Sc2O3	6.902349	7.3625056	3.527867248
V	36.7	43.3	4.9	V2O3	53.990252	63.69967	7.208507715
Ba	1426.8	1064.3	93.7	BaO	1593.0211	1188.2901	104.615975
Rb	85	97.1	78.6	Rb2O	92.956008	106.18857	85.95696736
Sr	394.3	424.7	18.2	SrO	466.30183	502.25307	21.52344214
Zr	127.5	136.3	314.8	ZrO2	172.22703	184.11408	425.2319228
Y	17.5	15.1	62.3	Y2O3	22.224144	19.176261	79.11795175
Nb	16	16	25.6	Nb2O5	22.888683	22.888683	36.6218931
Ga	16.7	17.3	18.6	Ga2O3	22.448709	23.25525	25.00275387
Cu	11	12.2	0	CuO	13.769647	15.271791	0
Zn	36.6	43.4	86.7	ZnO	45.840966	54.357866	108.5904845
Pb	21.1	23.3	20.3	PbO	22.729422	25.099315	21.86764323
La	44.7	49.5	33.7	La2O3	52.422986	58.0523	39.52247498
Ce	60.9	64.2	86.2	CeO2	74.861505	78.91804	105.9616055
Th	11.4	12.7	9.4	ThO2	12.579117	14.013578	10.37225454
Nd	31.9	30	51	Nd2O3	37.20782	34.991681	59.48585691
U	4.8	4.7	2.8	U2O3	5.2839726	5.1738898	3.082317355
				Cs2O	0	0	0
				As2O5	0	0	0
				W2O3	0	0	0

Notes

Major elements are normalized on a volatile-free basis, with total Fe expressed as FeO.

Sample locations (UTM coordinates; zone 13, NAD27)

djk-1015-1810: 403394 m E; 4039729 m N

djk1035-2210: 402945 m E, 4040998 m N

DJK-1030-1810: 403661 m E; 4040706 m N

Sample descriptions

DJK1015-1810: Rhyolitic flow breccia - lt purple and porphyritic. Phenocrysts=quartz, 20% plag and Kspar, and trace biotite.

DJK-1035-2210: Rhyolitic flow breccia - Gray to lt reddish gray. Phenocrysts=3% hornblende and biotite; 15% Kspar and sanidine.

DJK-1030-1810: White rhyolite pod. Gray to pinkish white. Abundant phenocrysts of smoky quartz.